J Biol Inorg Chem (2011) 16:235–242
DOI 10.1007/s00775-010-0720-4

ORIGINAL PAPER

Bacterial ferrochelatase turns human: Tyr13 determines the apparent metal specificity of *Bacillus subtilis* ferrochelatase

Mattias D. Hansson · Tobias Karlberg · Christopher A. G. Söderberg · Sreekanth Rajan · Martin J. Warren · Salam Al-Karadaghi · Stephen E. J. Rigby · Mats Hansson

Received: 18 June 2010 / Accepted: 9 October 2010 / Published online: 4 November 2010

Abstract Ferrochelatase catalyzes the insertion of Fe^{2+} into protoporphyrin IX. The enzymatic product heme (protoheme IX) is a well-known cofactor in a wide range of proteins. The insertion of metal ions other than Fe^{2+} occurs rarely in vivo, but all ferrochelatases that have been studied can insert Zn^{2+} at a good rate in vitro. Co^{2+}, but not Cu^{2+}, is known to be a good substrate of the mammalian and *Saccharomyces cerevisiae* ferrochelatases. In contrast, Cu^{2+}, but not Co^{2+}, has been found to be a good substrate of bacterial *Bacillus subtilis* ferrochelatase. It is not known how ferrochelatase discriminates between different metal ion substrates. Structural analysis of *B. subtilis* ferrochelatase has shown that Tyr13 is an indirect ligand of Fe^{2+} and a direct ligand of a copper mesoporphyrin product. A structure-based comparison revealed that Tyr13 aligns with a Met residue in the *S. cerevisiae* and human ferrochelatases. Tyr13 was changed to Met in the *B. subtilis* enzyme by site-directed mutagenesis. Enzymatic measurements showed that the modified enzyme inserted Co^{2+} at a higher rate than the wild-type *B. subtilis* ferrochelatase, but it had lost the ability to use Cu^{2+} as a substrate. Thus, the *B. subtilis* Tyr13Met ferrochelatase showed the same metal specificity as that of the ferrochelatases from *S. cerevisiae* and human.

Keywords Cobalt · Copper · Ferrochelatase · *hemH* · Metal specificity

Abbreviations
EPR Electron paramagnetic resonance
PDB Protein data bank

An interactive 3D complement page in Proteopedia is available at http://proteopedia.org/wiki/index.php/Journal:JBIC:4.

Electronic supplementary material The online version of this article (doi:10.1007/s00775-010-0720-4) contains supplementary material, which is available to authorized users.

M. D. Hansson · T. Karlberg · C. A. G. Söderberg · S. Rajan · S. Al-Karadaghi
Department of Biochemistry and Structural Biology,
Center for Molecular Protein Science,
Lund University, Box 124,
221 00 Lund, Sweden

M. J. Warren
Department of Biosciences,
University of Kent,
Canterbury CT2 7NJ, UK

S. E. J. Rigby
Manchester Interdisciplinary Biocentre,
University of Manchester,
131 Princess Street,
Manchester M1 7DN, UK

M. Hansson (✉)
Carlsberg Laboratory,
Gamle Carlsberg Vej 10,
2500 Valby, Copenhagen, Denmark
e-mail: mats@crc.dk

Introduction

Chelatases are a class of enzymes that catalyze the insertion of divalent metal ions into various tetrapyrroles. Among these are ferrochelatase (i.e., an iron chelatase) and the magnesium, cobalt, and nickel chelatases. Ferrochelatase catalyzes the final step in the synthesis of heme (protoheme IX), which is the insertion of Fe^{2+} into protoporphyrin IX [1, 2]. The protein is encoded by *hemH* and has been found in most species, since heme is essential for

a large number of biochemical processes. The factors that determine the metal specificity of different chelatases remain largely unknown. In the case of ferrochelatase, which is the best-studied chelatase, metal specificity has been addressed in a number of in vitro studies [1, 2]. It was found that the enzyme is promiscuous in vitro and could insert Zn^{2+}, Co^{2+}, Cu^{2+}, and Ni^{2+} into protoporphyrin IX in addition to the physiological substrate Fe^{2+} [1, 2]. Although insertion of divalent metal ions other than Fe^{2+} occurs only rarely in vivo, the formation of zinc protoporphyrin in connection to lead poisoning was observed [3, 4]. Interestingly, metal specificity of the ferrochelatase reaction appears to differ between enzymes from different host species. Fe^{2+}, Zn^{2+}, and Co^{2+}, but not Cu^{2+}, are known to be good substrates of *Saccharomyces cerevisiae* and mammalian ferrochelatases [5, 6]. On the other hand, Co^{2+} has been found to be a poor substrate of the bacterial *Bacillus subtilis* ferrochelatase, which instead has the ability to insert Cu^{2+} into protoporphyrin IX at a significant rate [7].

An analysis of ferrochelatase amino acid sequences from different species reveals that there are relatively few invariant amino acid residues across all species (Fig. 1). Many of these residues are Gly and Pro residues, which are typically found in regions between secondary structural elements and are known to be important for the preservation of the three-dimensional structure within a protein family [8–10]. The remaining residues are almost exclusively located in the active-site region, where, as shown by X-ray crystallographic studies, they interact with the metal ion substrate, the porphyrin substrate, or both [11–13]. In the case of *B. subtilis* ferrochelatase, metal soaking of the crystals and subsequent structure determination has shown that the physiological substrate Fe^{2+} is bound in a square-pyramidal geometry, coordinated to the invariant His183 and Glu264 residues, and via water molecules to Tyr13 and

```
B.SUB   ---------MSRKKMGLLVMAYGTPYKEEDIERYYTHIRR-----------------GRKPEPEMLQDLK   44
B.ANT   ----------MKKKIGLLVMAYGTPYKEEDIERYYTHIRR-----------------GRKPSPEMLEDLT   43
S.CER   -------NAQKRSPTGIVLMNMGGPSKVEETYDFLYQLFADNDLIPISAKYQKTIAKYIAKF--RTPKIE   92
HUMAN   GAKPQVQPQKRKPKTGILMLNMGGPETLGDVHDFLLRLFLDRDL--MTLPIQNKLAPFIAKR--RTPKIQ  120
                                 ^

B.SUB   DRYEAIGGISPLAQITEQQAHNLEQHLNEIQDEI-TFKAYIGLKHIEPFIEDAVAEMHKDGITEAVSIVL  113
B.ANT   ERYRAIGGISPLATITLEQAKKLEKRLNEVQDEVE-YHMYLGLKHIEPFIEDAVKEMHNDGIQDAIALVL  112
S.CER   KQYREIGGGSPIRKWSEYQATEVCKILDKTCPETAPHKPYVAFRYAKPLTAETYKQMLKDGVKKAVAFSQ  162
HUMAN   EQYRRIGGGSPIKIWTSKQGEGMVKLLDELSPNTAPHKYYIGFRYVHPLTEEAIEEMERDGLERAIAFTQ  190

B.SUB   APHFSTFSVQSYNKRAKEEAE---KLGGLTITSVESWYDEPKFVTYWVDRVKETYASMPEDERENAMLIV  180
B.ANT   APHYSTFSVKSYVGRAQEEAE---KLGNLTIHGIDSWYKEPKFIQYWVDAVKSIYSGMSDAEREKAVLIV  179
S.CER   YPHFSYSTTGSSINELWRQIKALDSERSISWSVIDRWPTNEGLIKAFSENITKKLQEFPQPVRDKVVLLF  232
HUMAN   YPQYSCSTTGSSLNAIYRYYNQVGRKPTMKWSTIDRWPTHHLLIQCFADHILKELDHFPLEKRSEVVILF  260

B.SUB   SAHSLPEKIKEFGDPYPDQLHESAKLIAEGAG-VSEYAVGWQSEGNTPDPWLGPDVQDLTRDLFEQKGYQ  249
B.ANT   SAHSLPEKIIAMGDPYPDQLNETADYIARGAE-VANYAVGWQSAGNTPDPWIGPDVQDLTRELNEKYGYT  248
S.CER   SAHSLPMDVVNTGDAYPAEVAATVYNIMQKLKFKNPYRLVWQSQVG-PKPWLGAQTAEIAEFLGP--KVD  299
HUMAN   SAHSLPMSVVNRGDPYPQEVSATVQKVMERLEYCNPYRLVWQSKVG-PMPWLGPQTDESIKGLCER-GRK  328
     ^

B.SUB   AFVYVPVGFVADHLEVLYDNDYECK-VVTDDIGA-SYYRPEMPNAKPEFIDALATVVLKKLGR-------  310
B.ANT   SFVYAPVGFVAEHLEVLYDNDFECK-VVTDEIGA-KYYRPEMPNASDAFIDCLTDVVVKKKESVM-----  311
S.CER   GLMFIPIAFTSDHIETLHEIDLGVIGES---EYKDKFKRCESLNGNQTFIEGMADLVKSHLQSNQLYSNQ  366
HUMAN   NILLVPIAFTSDHIETLYELDIEYSQVLAKECGVENIRRAESLNGNPLFSKALADLVHSHIQSNELCSKQ  398
                        ^

B.SUB   ----------------------------  310
B.ANT   ----------------------------  311
S.CER   LPLDFALGKSNDPVKDLSLVFGNHEST  393
HUMAN   LTLSCPLCVNPVCRETKSFFTSQQL--  423
```

Fig. 1 Alignment of structurally determined ferrochelatases: *Bacillus subtilis* [Protein Data Bank (PDB) code 1DOZ], *Bacillus anthracis* (PDB code 2C8J), *Saccharomyces cerevisiae* (PDB code 1LBQ), and human (PDB code 2QD4). The amino-terminal targeting sequence has been removed from the eukaryotic sequences. The alignment was done using the method of combinatorial extension [44]. The Tyr in the *B. subtilis* and *B. anthracis* ferrochelatases and the corresponding Met in the yeast and human enzymes have been marked with an *arrow*. *Arrows* are also used to mark the conserved His and Glu residues (numbers 183 and 264 in the *B. subtilis* sequence), which are direct ligands to the metal ion substrate. The *B. subtilis* ferrochelatase is 73, 24, and 28% identical to the *B. anthracis*, *S. cerevisiae*, and human ferrochelatases, respectively

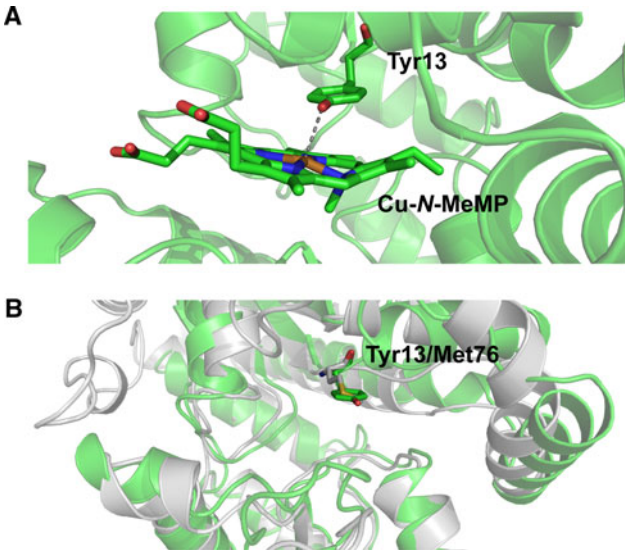

Fig. 2 **a** Copper *N*-methylmesoporphyrin bound in the active site of wild-type *B. subtilis* ferrochelatase, showing Tyr13 as the axial ligand of the metal ion (PDB code 1C9E). **b** Structural alignment of *B. subtilis* (*green*) and human (*gray*) ferrochelatases, showing Tyr13 and Met76 overlapping in an alignment with an overall root mean square deviation [25] of 2.0 Å (PDB codes 1DOZ and 2QD4)

the carbonyl group of Ser222 [11]. In a copper *N*-methylmesoporphyrin IX or copper mesoporphyrin IX complex with *B. subtilis* ferrochelatase, the copper ion is coordinated directly by Tyr13 and by the porphyrin nitrogen atoms (Fig. 2a) [14, 15]. Interestingly, Tyr13 is the only residue involved in Fe^{2+} binding that is not conserved. A structure-based alignment of ferrochelatase sequences revealed that at the position of Tyr13 in the *B. subtilis* enzyme, Met is present in the corresponding enzymes from *S. cerevisiae* [9] and humans [16] (Figs. 1, 2b). To assess the role of Tyr13 in the metal specificity of ferrochelatase, we performed site-directed mutagenesis of the *B. subtilis* enzyme to change this Tyr residue to a Met residue.

Materials and methods

Expression and purification of ferrochelatase

The wild-type and modified *B. subtilis* ferrochelatases were expressed in *Escherichia coli* BL21(DE3) and purified from inclusion bodies as described by Hansson et al. [17].

Site-directed mutagenesis

Site-directed mutagenesis was performed according to the QuikChange method (Stratagene) on plasmid pLUGT7-H, which contains the *B. subtilis hemH* gene downstream of an inducible T7 promoter [18]. The following primers were used: 5′-gcttctcgtgatggcgatgggcacgcctta-3′ (BsY13Mup1) and 5′-ccttataaggcgtgcccatcgccatcacga-3′ (BsY13MLo2). The mismatches introduced are underlined. The plasmid was named pLUGT7-HY13M. The correct DNA sequence was confirmed by sequencing.

X-ray crystallography

Initial crystals of Tyr13Met-modified ferrochelatase were found by screening under conditions in which wild-type crystallization was achieved [18]. The initial crystals were optimized further using seeding techniques as described earlier [18]. The crystal was transferred to a drop containing well solution supplemented with 10% PEG 400 as a cryoprotectant. A nylon loop was used to mount the crystal and flash-freeze it in a stream of boiled-off nitrogen. Diffraction data were collected at the MAX II synchrotron radiation facility in Lund, Sweden [19]. Data were indexed and integrated in space group $P2_12_12_1$ with the XDS package [20]. Pseudo-merohedral twinning was detected using Detwin in the CCP4 package [21]. The twinning fraction was estimated to be 15% and did not hamper the structural determination. The structure was initially refined using simulated annealing in CNS [22], and at later stages in Refmac5 [23]. The models were built using the graphics program Coot [24]. The progress of refinement was followed by monitoring decreasing R and R_{free} values. The statistics for data collection and refinement are shown in Table 1. The structure of the Tyr13Met-modified ferrochelatase has the Protein Data Bank (PDB) code 3GOQ.

Soaking of wild-type ferrochelatase crystals was conducted by transferring a crystal to a drop containing 10 µl of well solution supplemented with 5 mM $CoCl_2$, and incubating the mixture for 30 min. After soaking, the ferrochelatase crystal was transferred to another drop containing well solution with 10% PEG 400 as a cryoprotectant and mounted as described earlier. Data were collected and processed with the XDS package as described earlier. The twinning fraction was similar to that mentioned earlier, and the structure was solved using the structure of the wild-type enzyme for initial phasing. Data collection and refinement statistics are shown in Table 1. The PDB code for the structure is 3M4Z.

Enzymatic activity measurements

Two 40-ml portions were taken from a master mix consisting of 100 mM tris(hydroxymethyl)aminomethane–HCl, pH 7.4, 0.3 mg/ml Tween 80, and 1 µM protoporphyrin IX (Sigma). Wild-type or Tyr13Met-modified ferrochelatase was added to one of the portions to a final concentration of 0.05 µM. The other 40 ml was used for the negative controls without any enzyme added. A Tecan

Table 1 Statistics for the collected data and quality parameters for the refined structure of the modified Tyr13Met *B. subtilis* ferrochelatase and the wild-type (*WT*) ferrochelatase soaked in Co^{2+}

	Tyr13Met	WT soaked in Co^{2+}
Data collection		
Beamline	MAX II I911-5	MAX II I911-2
Wavelength (Å)	0.97935	1.03938
Space group	$P2_12_12_1$	$P2_12_12_1$
Cell dimensions		
a, *b*, *c* (Å)	48.33, 49.90, 118.05	48.41, 49.90, 118.08
α, β, γ (°)	90, 90, 90	90, 90, 90
Resolution (Å)	25.0–1.60 (1.69–1.60)	30–1.94 (1.99–1.94)
R_{merge} [a]	0.11 (0.42)	0.10 (0.51)
$\langle I/\sigma I \rangle$	13.0 (4.5)	22.7 (6.2)
Completeness (%)	97.7 (93.7)	99.9 (100)
Redundancy	7.1 (7.3)	13.5 (13.5)
Refinement		
Resolution (Å)	24.2–1.60 (1.64–1.60)	20–1.94 (1.99–1.94)
No. of reflections	35,770 (2,388)	20,726 (1,484)
R_{cryst} [b]/R_{free} [c]	0.1978 (0.2325)	0.1684 (0.1985)
RMSD [d]		
Bond lengths (Å)	0.012	0.012
Bond angles (°)	1.374	1.248
Ramachandran outliers [e]	0	0
Ramachandran favored (%) [e]	97.4	97.7

Values in *parentheses* are for the highest-resolution shell

RMSD root mean square deviation

[a] $R_{merge} = \sum|I_i - \langle I \rangle|/\sum I$, where I_i is an individual intensity measurement and $\langle I \rangle$ is the average intensity for this reflection

[b] $R_{cryst} = \sum|F_{obs} - F_{calc}|/\sum F_{obs}$, where F_{obs} and F_{calc} are the observed and calculated structure factor amplitudes, respectively

[c] R_{free} is the same as R_{cryst} but calculated on 5% of the data excluded from refinement

[d] RMSDs of the parameters from their ideal values

[e] According to Molprobity structure validation [43]

robot system (Tecan Group, Switzerland) was used to transfer 2-ml portions of the mixtures, either containing or not containing ferrochelatase, into a deep 96-well plate. The activity with Cu^{2+}, Co^{2+}, and Zn^{2+} was analyzed. Twenty microliters of $CuCl_2$, $CoCl_2$, or zinc acetate solutions was added to the 2-ml portions, resulting in metal ion concentrations of between 0.25 and 200 μM. The 2-ml portions were aliquoted in 300-μl portions in black 96-well plates. Every second column contained the negative control samples without any ferrochelatase. For each metal ion concentration, six replicates were assayed. Since only zinc protoporphyrin IX is fluorescent, and not cobalt protoporphyrin IX and copper protoporphyrin IX, the enzymatic activities were followed from the reduction in protoporphyrin IX substrate. One unit of protoporphyrin IX consumed per minute and milligram of protein was regarded as equivalent to the formation of one unit of the corresponding metal ion protoporphyrin IX per minute and milligram of protein. Every 30 min over a 6-h period, the black 96-well plates were moved to a Magellan M200 plate reader (Tecan Group, Switzerland) connected to the robot system. The decrease in protoporphyrin IX was monitored using an excitation wavelength of 511 nm (slit 9 nm) and an emission wavelength of 637 nm (slit 20 nm). All operations were performed in the dark owing to the light sensitivity of protoporphyrin IX. Assays without added enzymes were used as controls and the spontaneous incorporation of metal ion into protoporphyrin IX was subtracted. The first time points at 0 min were omitted from the evaluations to avoid pre-steady-state conditions.

EPR spectroscopy

EPR spectra were measured at X-band (approximately 9.5 GHz) using a Bruker ELEXSYS E500 spectrometer fitted with an Oxford Instruments ESR900 cryostat to allow measurements to be made at cryogenic temperatures using liquid helium vapor. Temperature control was achieved using an Oxford Instruments ITC503 temperature controller. The experimental parameters were as follows: microwave power 0.5 mW, modulation amplitude 5 G, and temperature 15 K.

Results

Metal-specific activity of wild-type and Tyr13Met-modified ferrochelatase

Site-directed mutagenesis was performed on *hemH* to change Tyr13 to Met in the resulting protein. The plasmid carrying the mutated *hemH* was named pLUGT7-HY13M. The entire gene was sequenced from both strands to verify the mutation and to verify that the remainder of the gene was intact. The wild-type and Tyr13Met-modified ferrochelatases were produced in *E. coli* BL21(DE3) and purified from inclusion bodies as described earlier [17]. Tyr13Met-modified ferrochelatase was crystallized with the microseeding technique used for the wild-type ferrochelatase [18]. Diffraction data to a resolution of 1.6 Å were collected (Table 1). The final coordinates were deposited in the PDB (accession code 3GOQ). Although the Met residue replaced the Tyr residue in the active site, the overall structure was found to be very similar to that of wild-type *B. subtilis* ferrochelatase, with a root mean square deviation [25] between the Cα atoms of 0.2 Å (Fig. 3).

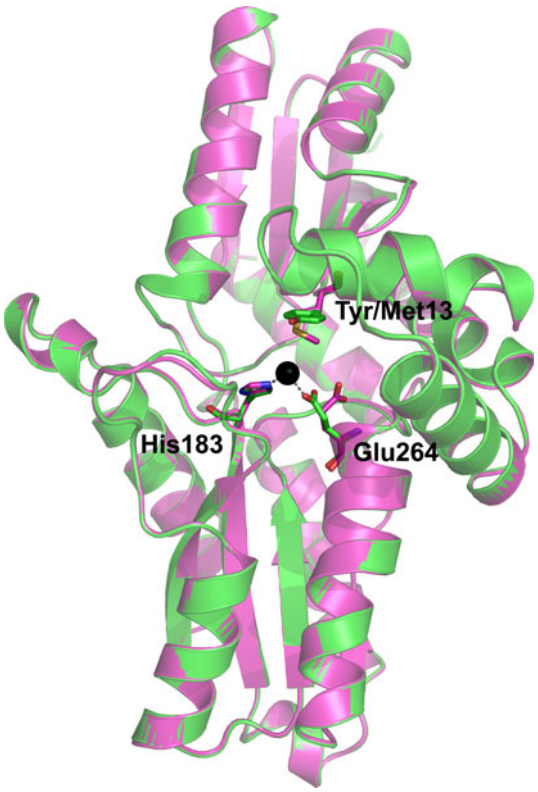

Fig. 3 Structural alignment of wild-type *B. subtilis* ferrochelatase with bound Fe^{2+} (*black sphere*) (PDB code 2HK6, *green*) and the Tyr13Met-modified enzyme (PDB code 3GOQ, *magenta*). His183 and Glu264 are the only direct ligands of the iron. The only notable movement is that of Glu264, which is due to the binding of Fe^{2+}. The overall root mean square deviation is 0.2 Å. It should be noted that structures of *B. subtilis* ferrochelatase in complex with Fe^{2+} (2HK6), Zn^{2+} (1LD3), and Co^{2+} (3M4Z) are all very similar and have the metal ions positioned at the same site

Activity measurements showed that wild-type *B. subtilis* ferrochelatase inserts Cu^{2+} into protoporphyrin IX at a rate of 110 pmol/(min mg ferrochelatase) with a K_M of 63 μM (Figs. 4, S1). The activity with Zn^{2+} was 10 times higher: 1,100 pmol/(min mg ferrochelatase), with a K_M of 13 μM. This activity is in good agreement with the activity reported earlier for the *B. subtilis* ferrochelatase with Zn^{2+} [26]. With the modified enzyme with Met at position 13, no formation of copper protoporphyrin IX or zinc protoporphyrin IX could be detected, i.e., the activity of the enzyme was less than 4.2 pmol/(min mg ferrochelatase). In contrast, cobalt protoporphyrin IX was formed at a rate of 57 pmol/(min mg ferrochelatase), which is higher than the activity of the wild-type enzyme with the same metal as the substrate [27 pmol/(min mg ferrochelatase)]. A change of Tyr13 to Met is, however, a severe modification of *B. subtilis* ferrochelatase and the K_M of 560 μM is considerably higher than the K_M of the wild-type enzyme (5.2 μM) with Co^{2+} as substrate. Clearly, the Tyr13Met modification of *B. subtilis* ferrochelatase changes the metal specificity of

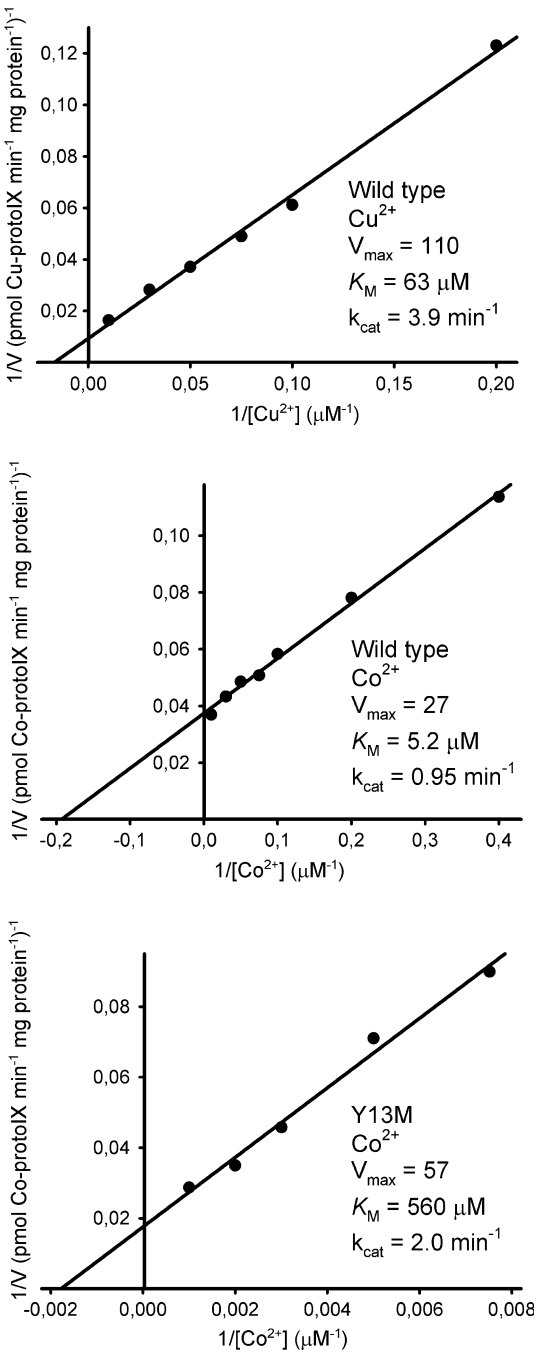

Fig. 4 Lineweaver–Burk plots of wild-type and Tyr13Met-modified *B. subtilis* ferrochelatase with Cu^{2+} or Co^{2+} as the substrate. The modified ferrochelatase could insert Co^{2+} into protoporphyrin IX at a higher rate than the wild-type enzyme, but had lost the ability to insert Cu^{2+} and Zn^{2+}. *V* and V_{max} are expressed as picomoles of Cu^{2+} protoporphyrin IX/Co^{2+} protoporphyrin IX formed per minute and milligram of protein

the enzyme and results in preference for Co^{2+} over Cu^{2+} as the substrate. These results are in line with the metal specificity of the ferrochelatases from *S. cerevisiae* and mammals, which naturally have a Met residue in the active site at the position of Tyr13 in the *B. subtilis* enzyme.

Metal ion binding

The environment of the Cu^{2+} and Co^{2+} ions in the wild-type and Tyr13Met-modified ferrochelatases was studied using low-temperature X-band EPR spectroscopy. Cu^{2+} and Co^{2+} EPR spectra are sensitive reporters concerning the environment of the ion because the spin and orbital energies of the ion's unpaired electrons are affected by the arrangement and nature of the atoms ligating the ion. EPR spectroscopy has previously been used in metal-binding studies of Met8p from *S. cerevisiae*, a bifunctional dehydrogenase and ferrochelatase [27]. The Co^{2+} EPR spectra show one broad line at around $g = 4$, typical of mononuclear high spin; $S = 3/2$ for Co^{2+} axial systems with octahedral symmetry [28]. The high-spin state suggests that there are mainly, but not exclusively, oxygen ligands rather than nitrogen ligands in the immediate environment of the metal ion. For Co^{2+} in buffer without ferrochelatase, the spectrum appears at $g_{\perp} = 4.4$ with a half-height linewidth of 520 G (Fig. 5). In the presence of wild-type or Tyr13-Met-modified ferrochelatase, the spectrum shifts to $g_{\perp} = 4.3$ with a half-height linewidth of 600 G. There is also evidence of a weak $g_{\|}$ feature at $g \sim 3$ in all spectra, and further lines around $g = 2.0$–2.3 arise from contaminating Cu^{2+} in the EPR resonator. The Cu^{2+} EPR spectra are consistent with an $S = ½$ ground state bearing the unpaired electron in the $d_{x^2-y^2}$ orbital with distorted octahedral symmetry. For Cu^{2+} in buffer without enzyme, the axial spectrum has $g_{\perp} = 2.05$ with $g_{\|} = 2.25$ and $A_{\|} = 175$ G, whereas in the presence of wild-type or Tyr13Met-modified ferrochelatase we observed $g_{\perp} = 2.06$ with $g_{\|} = 2.27$ and $A_{\|} = 170$ G. A minor species with $g_{\|} = 2.22$ and $A_{\|} = 166$ G constituted about 10% of the observed Cu^{2+} signal. These spectra are consistent with a metal ion environment that is dominated by oxygen ligation, with one possible nitrogen ligand [29]. Overall, the EPR analysis demonstrates that the two metal ions are bound in identical fashion in the wild-type and the Tyr13Met enzymes (Fig. 5).

The mode of metal binding suggested by the EPR experiments was further confirmed by an X-ray crystallographic study of binding of Co^{2+} to ferrochelatase. Crystals of wild-type ferrochelatase were soaked in 5 mM $CoCl_2$ for 30 min. Difference electron density maps clearly demonstrated the presence of Co^{2+} at the active site of the enzyme (up to 10σ, Fig. 6). The metal was coordinated by the invariant amino acid residues His183 and Glu264, and by four water molecules in a distorted octahedral fashion. Tyr13 appears to stabilize one of the water molecules in the second coordination sphere of the metal. The position of the Co^{2+} ion in the structure is very similar to the binding positions seen earlier in both *B. subtilis* and *S. cerevisiae*

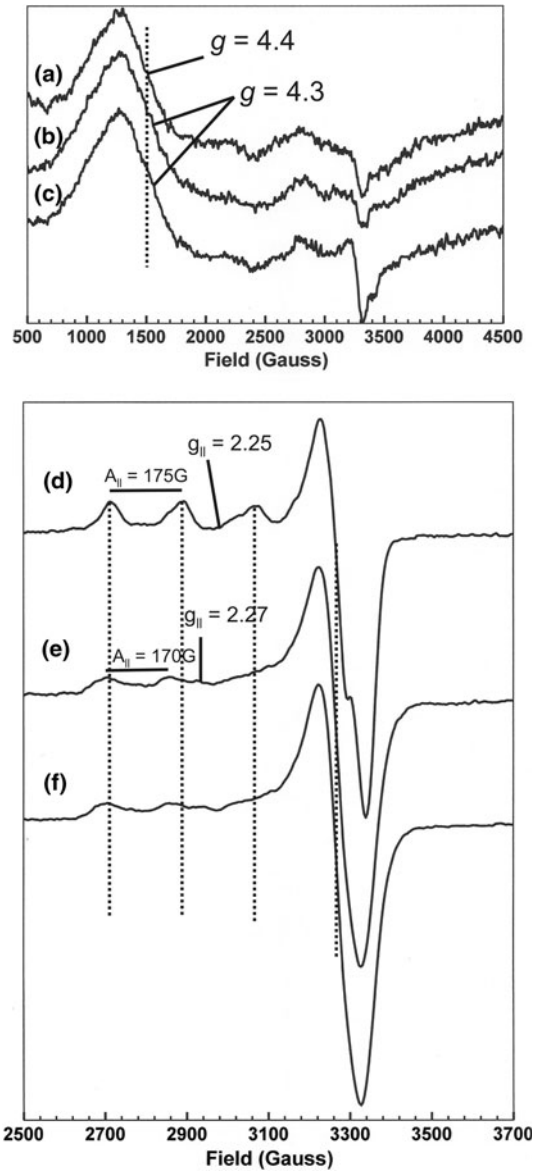

Fig. 5 X-band EPR spectra of ferrochelatases and metal ion controls (1 equiv is equal to the protein concentration): *a* 1 equiv of Co^{2+} ions in buffer; *b* 1 equiv of Co^{2+} ions with wild-type ferrochelatase; *c* 1 equiv of Co^{2+} ions with Tyr13Met-modified ferrochelatase; *d* 1 equiv of Cu^{2+} ions in buffer; *e* 1 equiv of Cu^{2+} ions with wild-type ferrochelatase; *f* 1 equiv of Cu^{2+} ions with Tyr13Met-modified ferrochelatase. Each spectrum was the co-added sum of three scans. The experimental parameters were as follows: microwave power 0.5 mW, modulation amplitude 5 G, temperature 15 K

ferrochelatase [9, 11, 26]. Moreover, three of the four water molecules in the Co^{2+} coordination sphere can be superimposed on all three water molecules in the Fe^{2+} coordination sphere. In addition, in the Co^{2+}-soaked structure, Mg^{2+}—which is essential for crystal formation and which has been observed in most *B. subtilis* crystal structures—remained 7.7 Å from the Co^{2+} ion (7.8 Å from Fe^{2+}). It is

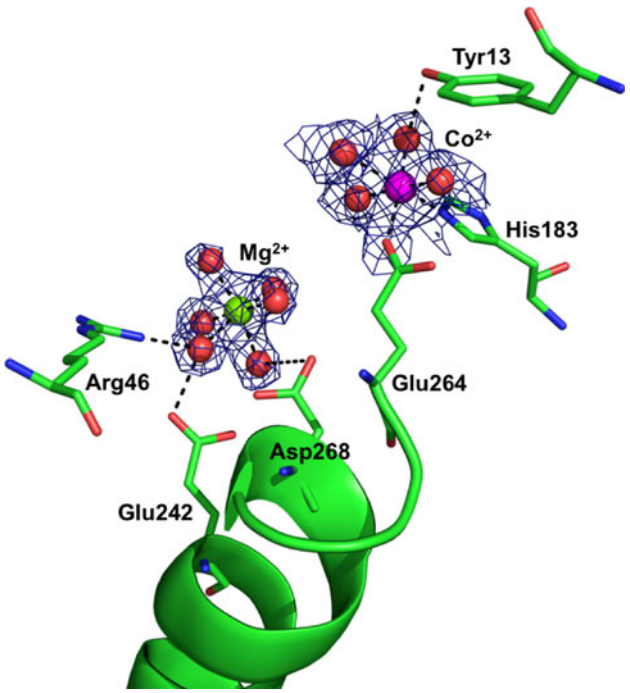

Fig. 6 Cobalt bound in the active site of *B. subtilis* ferrochelatase (PDB code 3M4Z). Co^{2+} is coordinated to His183, Glu264, and four water molecules. Tyr13 is an indirect ligand of Co^{2+} via water

interesting to note that Mg^{2+} is absent from the Zn^{2+}-soaked structure, which has been suggested to be an effect of repulsive interactions between the two metal ions [17].

Discussion

To assess the specificity of the metallation reaction catalyzed by ferrochelatase, we changed Tyr to Met at position 13 of the *B. subtilis* ferrochelatase using site-directed mutagenesis. The modified Tyr13Met enzyme could insert Co^{2+} into protoporphyrin IX at a higher rate than the wild-type enzyme, but no activity with Cu^{2+} and Zn^{2+} could be detected. Our experiments clearly demonstrate that the Tyr13Met substitution does indeed affect the metal specificity of the ferrochelatase reaction, although both EPR data and the X-ray crystallographic model of the Co^{2+}-soaked enzyme showed that both Cu^{2+} and Co^{2+} bind to *B. subtilis* ferrochelatase in a manner that is insensitive to the Tyr13Met substitution. Furthermore, we found that Co^{2+} binds to the same amino acid residues in the ferrochelatase structure as those used for Fe^{2+} and Zn^{2+} [11, 26]. These observations suggest that metal substrate specificity is not determined at the stage of binding of the metal ion to the enzyme, but rather at a later stage of the reaction. Are there any previous observations to support this suggestion? Distortion of the porphyrin ring is strongly believed to be a key feature of the ferrochelatase reaction mechanism [30–33]. Distorted porphyrins are also seen in X-ray crystallographic structures of ferrochelatase in complex with porphyrin [12, 14, 16]. The distortion is believed to serve the enzymatic reaction by exposing the nitrogen atoms of the porphyrin to the incoming metal ion. Recent kinetic studies on human ferrochelatase have demonstrated that product release in vitro is at least 10 times slower than metal insertion, which led to the conclusion that release of the product is the overall rate-limiting step in the reaction [34]. Theoretical simulations have shown that the energy required to distort a metallated porphyrin is normally higher than the energy required to distort an empty porphyrin. This means that the release of a metallated product is energetically favorable, and it suggests that the release mechanism may explore the differences in energy between a distorted metal-containing porphyrin and a metal-free porphyrin [32]. One exception is cadmium porphyrin, which requires less energy to be tilted than the neutral metal-free ring [32]. In accordance with theoretical calculations, it was found that Cd could be inserted into porphyrin by human ferrochelatase in vitro, but the product of the reaction, cadmium porphyrin, was retained by the enzyme [35]. These observations also support the idea that inhibition of the ferrochelatase reaction by metalloporphyrin may contribute to control of the metal substrate specificity of the enzyme. Combined, the present and previous studies suggest that ferrochelatase does not have the ability to discriminate between transition metal ion substrates in the binding phase of the reaction. Still, the overall ferrochelatase reaction shows metal specificity. We regard this metal specificity as apparent because it is related to the release of the product after the metal insertion into the porphyrin has been completed. How could a change of Tyr13 to Met in the *B. subtilis* ferrochelatase affect this apparent metal specificity of Cu^{2+} versus Co^{2+}? Our previous work has demonstrated that a His183Ala replacement in the active site of *B. subtilis* ferrochelatase affects the mode of porphyrin distortion, suggesting that the binding site of the enzyme is optimized for enforcing a certain type of distortion on the bound porphyrin [12]. It would be logical to assume that the binding site is also optimized for release of a certain metallated product. Our previous analysis has shown that Tyr13 is involved in binding of the metal ion substrate, but only as an indirect ligand mediated via water [26]. In contrast, Tyr13 is a direct ligand to the metal ion in copper *N*-methylmesoporphyrin IX and copper mesoporphyrin IX complexes [14, 15]. It can therefore be speculated that a Tyr or Met residue in the active site may influence the binding of a metalloporphyrin to a greater extent than it can influence the binding of the plain metal ion. It should be noted that Co^{2+} is a harder ion than Cu^{2+} [36]. Thus, cobalt protoporphyrin should have a stronger affinity for hard ligands, such as the oxygen of the hydroxyl

group of Tyr13, providing an axial ligand to the metalloporphyrin. Thus, the cobalt protoporphyrin product should be retained by Tyr13 in the *B. subtilis* ferrochelatase. Correspondingly, the softer copper in copper protoporphyrin should be retained more strongly by the softer sulfur of Met, negatively affecting the release of product from the Tyr13Met enzyme as well as from the *S. cerevisiae* and mammalian ferrochelatases.

Our study indicates that ferrochelatase does not have a built-in mechanism to discriminate between incoming transition metal ion substrates. Instead, an in vivo metal delivery system is likely to exist, one that is metal-specific and ensures the delivery of Fe^{2+} to ferrochelatase. Frataxin and mitoferrin have been suggested to function as Fe^{2+} chaperones of the ferrochelatase reaction [37–40]. No homologs can be found when prokaryotic genomes are screened in bioinformatic searches. Thus, it is uncertain whether they are Fe^{2+} chaperones that are universal for ferrochelatases of all species. Recently, however, Qi and Cowan [41] reported that the *B. subtilis* protein YdhG is structurally and functionally similar to frataxin, even though there was no sequence homology. The conserved residue Ser54 in the *B. subtilis* ferrochelatase has been suggested to be part of a docking site for a protein with the function of delivering any of the two substrates, or retrieving the heme product [42]. A future challenge will be to identify and understand the trafficking of substrates and product of ferrochelatase and the proteins that interact with it.

Acknowledgments We thank Ulf Ryde for insightful discussions. M.D.H. and C.A.G.S. acknowledge IRTG—Metal Sites in Biomolecules (http://www.biometals.eu). This work was supported by grants from the Royal Physiographical Society in Lund (M.D.H.), the Danish Natural Science Research Council (M.H.), the Swedish Research Council (M.H., S.A.K.), the Carlsberg Foundation (M.H.), the Crafoord Foundation (M.H., S.A.K.), and the Carl Trygger Foundation (S.A.K.).

References

1. Dailey HA, Dailey TA (2003) In: Kadish KM, Smith K, Guilard R (eds) The tetrapyrrole handbook II. Academic Press, San Diego, pp 93–122
2. Dailey HA, Dailey TA, Wu CK, Medlock AE, Wang KF, Rose JP, Wang BC (2000) Cell Mol Life Sci 57:1909–1926
3. Grandjean P, Lintrup J (1978) Scand J Clin Lab Invest 38:669–675
4. Lamola AA, Yamane T (1974) Science 186:936–938
5. Hunter GA, Sampson MP, Ferreira GC (2008) J Biol Chem 283:23685–23691
6. Taketani S, Tokunaga R (1982) Eur J Biochem 127:443–447
7. Hansson M, Hederstedt L (1994) Eur J Biochem 220:201–208
8. Al-Karadaghi S, Hansson M, Nikonov S, Jönsson B, Hederstedt L (1997) Structure 5:1501–1510
9. Karlberg T, Lecerof D, Gora M, Silvegren G, Labbe-Bois R, Hansson M, Al-Karadaghi S (2002) Biochemistry 41:13499–13506
10. Wu CK, Dailey HA, Rose JP, Burden A, Sellers VM, Wang BC (2001) Nat Struct Biol 8:156–160
11. Hansson MD, Karlberg T, Rahardja MA, Al-Karadaghi S, Hansson M (2007) Biochemistry 46:87–94
12. Karlberg T, Hansson MD, Yengo RK, Johansson R, Thorvaldsen HO, Ferreira GC, Hansson M, Al-Karadaghi S (2008) J Mol Biol 378:1074–1083
13. Medlock A, Swartz L, Dailey TA, Dailey HA, Lanzilotta WN (2007) Proc Natl Acad Sci USA 104:1789–1793
14. Lecerof D, Fodje M, Hansson A, Hansson M, Al-Karadaghi S (2000) J Mol Biol 297:221–232
15. Shipovskov S, Karlberg T, Fodje M, Hansson MD, Ferreira GC, Hansson M, Reimann CT, Al-Karadaghi S (2005) J Mol Biol 352:1081–1090
16. Medlock AE, Dailey TA, Ross TA, Dailey HA, Lanzilotta WN (2007) J Mol Biol 373:1006–1016
17. Hansson MD, Lindstam M, Hansson M (2006) J Biol Inorg Chem 11:325–333
18. Hansson M, Al-Karadaghi S (1995) Proteins 23:607–609
19. Mammen CB, Ursby T, Thunnissen M, Als-Nielsen J (2004) AIP Conf Proc 705:808–811
20. Kabsch W (1993) J Appl Crystallogr 26:795–800
21. Collaborative Computational Project N (1994) Acta Crystallogr D 50:760–763
22. Brunger AT, Adams PD, Clore GM, DeLano WL, Gros P, Grosse-Kunstleve RW, Jiang JS, Kuszewski J, Nilges M, Pannu NS, Read RJ, Rice LM, Simonson T, Warren GL (1998) Acta Crystallogr D 54:905–921
23. Murshudov GN, Vagin AA, Dodson EJ (1997) Acta Crystallogr D 53:240–255
24. Emsley P, Cowtan K (2004) Acta Crystallogr D 60:2126–2132
25. Shindyalov IN, Bourne PE (1998) Protein Eng 11:739–747
26. Lecerof D, Fodje MN, León RA, Olsson U, Hansson A, Sigfridsson E, Ryde U, Hansson M, Al-Karadaghi S (2003) J Biol Inorg Chem 8:452–458
27. Schubert HL, Rose RS, Leech HK, Brindley AA, Hill CP, Rigby SE, Warren MJ (2008) Biochem J 415:257–263
28. Bencini A, Benelli C, Gatteschi D, Zanchini C (1980) Inorg Chem 19:1301–1304
29. Peisach J, Blumberg WE (1974) Arch Biochem Biophys 165:691–708
30. Hambright P, Chock PB (1974) J Am Chem Soc 96:3123–3131
31. Lavallee DK (1988) Mol Struct Energ 9:279–313
32. Sigfridsson E, Ryde U (2003) J Biol Inorg Chem 8:273–282
33. Al-Karadaghi S, Franco R, Hansson M, Shelnutt JA, Isaya G, Ferreira GC (2006) Trends Biochem Sci 31:135–142
34. Hoggins M, Dailey HA, Hunter CN, Reid JD (2007) Biochemistry 46:8121–8127
35. Medlock AE, Carter M, Dailey TA, Dailey HA, Lanzilotta WN (2009) J Mol Biol 393:308–319
36. Williams RJP (1990) Coord Chem Rev 100:573–610
37. Lesuisse E, Santos R, Matzanke BF, Knight SA, Camadro JM, Dancis A (2003) Hum Mol Genet 12:879–889
38. Paradkar PN, Zumbrennen KB, Paw BH, Ward DM, Kaplan J (2009) Mol Cell Biol 29:1007–1016
39. Park S, Gakh O, O'Neill HA, Mangravita A, Nichol H, Ferreira GC, Isaya G (2003) J Biol Chem 278:31340–31351
40. Yoon T, Cowan JA (2004) J Biol Chem 279:25943–25946
41. Qi W, Cowan JA (2010) Chem Commun 46:719–721
42. Olsson U, Billberg A, Sjövall S, Al-Karadaghi S, Hansson M (2002) J Bacteriol 184:4018–4024
43. Lovell SC, Davis IW, Arendall WB 3rd, de Bakker PI, Word JM, Prisant MG, Richardson JS, Richardson DC (2003) Proteins 50:437–450
44. Guda C, Scheeff ED, Bourne PE, Shindyalov IN (2001) Pac Symp Biocomput 275–286